Antiferroelectricity in oxides: a reexamination

Karin M. Rabe*
Department of Physics and Astronomy
Rutgers University, Piscataway, NJ 08854
** Corresponding Author: rabe@physics.rutgers.edu*
(Dated: December 17, 2012)

The fundamental physics of antiferroelectric oxides and their properties are reviewed. First, the difficulties in formulating a precise definition of antiferroelectricity are discussed, drawing on previous discussion in the literature. We arrive at the following definition: *an antiferroelectric is like a ferroelectric in that its structure is obtained through distortion of a nonpolar high-symmetry reference phase; for ferroelectrics, the distortion is polar, while for antiferroelectrics it is nonpolar. However, not all nonpolar phases thus obtained are antiferroelectric: in addition, there must be an alternative low-energy ferroelectric phase obtained by a polar distortion of the same high-symmetry reference structure, and an applied electric field must induce a first-order transition from the antiferroelectric phase to this ferroelectric phase, producing a characteristic P-E double-hysteresis loop.* For analysis of the characteristic properties of antiferroelectrics, we use Landau theory functionals. The microscopic origins of the macroscopic behavior are examined. This is fairly straightforward for systems with clearly-defined reorientable local-dipolar entities, such as antiferroelectric liquid crystals and hydrogen-bonded antiferroelecrics, and these systems are not discussed in any detail in this article. The main focus is on the subtler case of antiferroelectric oxides, for which models based on symmetry-adapted lattice modes prove to be useful. Specific examples of antiferroelectric oxides are presented with available first principles results and discussion of the role of compositional tuning in producing antiferroelectricity, and the nature of the electric-field-induced ferroelectric phases. In thin films and superlattices, additional tuning is possible through the effects of strain and finite size. The article concludes with some remarks on materials design, including the optimization of properties relevant to technological applications of antiferroelectrics.

PACS numbers: 81.05.Zx

INTRODUCTION

As the result of progress both in synthesis and in first-principles studies, there has been a lot of interest and progress in the investigation and rational design of functional materials with enhanced or novel properties [1–8]. Insofar as functional properties arise from coupling to macroscopic fields and stresses, attention has focused on ferroic materials: ferromagnets, ferroelectrics, piezoelectrics, and multiferroic combinations, with order parameters that have macroscopic conjugate fields. The potential of antiferroic materials for functional properties is less obvious, since an antiferroic order parameter does not couple directly to a macroscopic field, but rather to a microscopic staggered field. However, such materials can also exhibit characteristic functional behavior in applied macroscopic fields. Antiferromagnets have been well-studied [9]. Here, we consider the electric analogue: antiferroelectrics. The definition of antiferroelectricity is in general more subtle than for antiferromagnets, as only certain classes of materials have well-defined localized electric dipoles that can be regarded as analogues of the local magnetic moments in antiferromagnets. In this paper, these materials, which include hydrogen-bonded antiferroelectrics and antiferroelectric liquid crystals, will not be discussed. Rather, the focus is on antiferroelectricity in oxides, which requires a more broadly applicable definition of antiferroelectricity and criteria for establishing a material as antiferroelectric.

As will be discussed more fully below, antiferroelectrics are characterized by an antipolar crystal structure with a related ferroelectric polar structure at low free energy. As recognized by Shirane in the earliest studies of antiferroelectric perovskite oxides [10, 11], the competition between ferroelectric and antiferroelectric phases is an intrinsic feature of antiferroelectrics (Figure 1). The free energy difference is in general tunable in a variety of ways, including composition substitution, epitaxial strain and size effects. Therefore, proximity to ferroelectric phases though a first-order phase boundary in the phase diagram is an important indication of antiferroelectricity. The most characteristic property resulting from the low free-energy difference is the electric-field induced transition from the antiferroelectric to the related ferroelectric state in a double hysteresis loop (Figure 2). In systems where the two phases have different cell volume or shape, this transition is accompanied by large nonlinear strain responses. Other characteristic properties include dielectric anomalies at the antiferroelectric-paraelectric transition in zero field, large electrostriction coefficients and giant electrocaloric effects [13, 14]. The types of applications this functionality would enable [15–17] include high-energy storage capacitors, electrocaloric refrigerators, high-strain actuators and transducers. For

FIG. 1: Schematic free energy curves for antiferroelectric $PbZrO_3$, showing the presence of a low-free-energy alternative ferroelectric phase. From Ref. [11].

FIG. 2: Double hysteresis loop for $PbZrO_3$, as redrawn in Ref. [12] from Ref. [10].

realization of these applications, a number of materials properties, including operating temperature, critical electric fields, strain change at the field-induced transition, and switching time and reversibility of the field-induced transition, need to be optimized. This tuning is accomplished largely through compositional substitution, leading to multi-component materials with complex stoichiometries.

In this article, I review aspects of the fundamental physics of antiferroelectric materials and their properties. First, the difficulties in formulating a precise definition of antiferroelectricity are discussed, drawing on previous discussion in the literature. For analysis of the characteristic properties of antiferroelectrics, we use Landau theory functionals. The microscopic origins of the macroscopic behavior are examined. This is fairly straightforward for systems with clearly-defined reorientable local-dipolar entities, such as antiferroelectric liquid crystals and hydrogen-bonded antiferroelecrics, and these systems are not discussed in any detail in this article. The main focus is on the subtler case of antiferroelectric oxides, for which models based on symmetry-adapted lattice modes prove to be useful. Specific examples of antiferroelectric oxides are presented with available first principles results and discussion of the role of compositional tuning in producing antiferroelectricity, and the nature of the electric-field-induced ferroelectric phases. In thin films, additional tuning is possible through the effects of strain and finite size. The article concludes with some remarks on materials design, including the optimization of properties relevant to technological applications of antiferroelectrics.

DEFINITION AND CHARACTERISTIC PROPERTIES

According to the standard reference book by Lines and Glass [18], an antiferroelectric is a phase obtained by condensation of a nonpolar lattice mode which "exhibits large dielectric anomalies near the transition temperature and which can be transformed to an induced ferroelectric phase by application of an electric field." A similar definition, emphasizing that the concept of antiferroelectricity is "based not only upon the crystal structure, but also upon the dielectric behavior of the crystal," appears in a recent overview article in Landolt Bornstein [19]. There is a close analogy to the definition for a ferroelectric as a phase obtained by condensation of a polar lattice mode, which can be switched between two or more symmetry-related variants by an applied electric field. These definitions of both ferroelectrics and antiferroelectrics are often extended to include the possibility that the transition temperature is above the decomposition temperature of the material, or that the critical electric field is above (but not too far above) the breakdown field of the material. The definition clearly distinguishes antiferroelectrics from the much larger group of materials with centrosymmetric structures which can be described by unit cells with oppositely directed dipoles generated by ionic displacements from a higher-symmetry reference structure, but without any distinctive behavior in applied electric field.

Other formulations of the definition of antiferroelectricity are more closely based on the analogy to antiferromagnetism, with a staggered electric polarization playing the role of the staggered magnetization. In the simplest cases, the formulation of the staggered polarization involves identification in the crystal structure of two (or more) symmetry-related sublattices of polarized ions or molecular units with opposite polarization; this is, in essence, the definition introduced in 1951 by Kittel [20] An energetic criterion was subsequently added to this

structure-based definition by Shirane [10, 11], yielding a definition of an antiferroelectric [21] as an antipolar crystal whose free energy is comparable to that of the polar crystal obtained by aligning the sublattice polarizations. This extends the analogy to antiferromagnetism, with a transition to a ferroelectric phase being induced by an applied electric field.

The importance of both structural and energetic aspects of the definition of antiferroelectrics can be made clear using a Landau energy functional formulation. Using the concept of a well-defined sublattice polarization as a starting point, Kittel [20] established some characteristic properties of antiferroelectrics by introducing the free energy expression

$$A(P_a, P_b, T) = A_0 + f(P_a^2 + P_b^2) + gP_aP_b + h(P_a^4 + P_b^4) + j(P_a^6 + P_b^6) - (P_a + P_b)E \quad (1)$$

where P_a and P_b are the polarizations of two sublattices and E is the electric field, with $g > 0$ favoring the antipolar alignment of the two sublattices. This can be transformed into a Landau functional [22–24]

$$G_1(P_F, P_A, T) = (1/2)(f + g/2)P_F^2 + (1/2)(f - g/2)P_A^2 + (h/8)(P_F^4 + 6P_A^2P_F^2 + P_A^4) + \mathcal{O}(P^6) - P_FE \quad (2)$$

where $P_F = P_a + P_b$ is the macroscopic polarization and $P_A = P_a - P_b$ is the staggered polarization. Temperature dependence is introduced into the quadratic coefficients as $f(T) = g/2 + \lambda(T - T_c)$, so that the quadratic coefficient of P_A vanishes at T_c and $\lambda > 0$ corresponds to a low-temperature antiferroelectric phase. The temperature dependences of the quadratic terms in P_F and P_A are linked, as are the quartic coefficients, by the original two-sublattice model. Depending on the choice of parameters, the transition can be first or second order. For a second order transition, $h > 0$ and the sixth order terms can be neglected. There is a phase transition from the high-temperature phase to the antiferroelectric phase at T_c, below which the spontaneous polarization of the sublattices and thus P_A become nonzero. The temperature dependence of the dielectric constant is such that it is a maximum at the Curie temperature and changes slope slightly. For a first order transition, $h < 0$ and $j > 0$, and there will be a discontinuity in the sublattice polarization and the dielectric constant at the paraelectric-antiferroelectric transition.

Using this function, the analysis of the behavior in applied electric field is straightforward [22–24]. For values of the parameters giving antiferroelectric states in zero field, double hysteresis loops are obtained, corresponding to the loss of local stability of the higher energy state. This assumption yields a hysteresis loop that will in general be wider than would be expected in a real system, where more complex switching mechanisms may allow the system to overcome the barrier to the lower-free-energy phase before the loss of local stability of the higher energy state. Antiferroelectrics also exhibit an electrocaloric effect, with a change in temperature with applied field under adiabatic conditions [13], which can be described with a thermodynamic analysis.

In addition to characteristic electrical properties, antiferroelectrics exhibit characteristic properties related to coupling of the sublattice polarizations to strain; polarization-strain coupling is significant in many perovskite ferroelectrics [25]. Most nonpolar space groups forbid piezoelectricity (one exception being $P4\bar{3}m$) and therefore most antiferroelectrics are not piezoelectric. Symmetry does not forbid electrostriction. A change in the temperature dependence of the lattice parameters, with an accompanying effect on dielectric properties, is generally observed at the transition from the antiferroelectric to the paraelectric phase. There is also generally a lattice parameter change at the electric-field-induced antiferroelectric-ferroelectric transition; in $PbZrO_3$, this takes the form of a large volume expansion [26]. In that case, the transition back to the antiferroelectric state can also be driven by compressive stress at fields close to the critical field [27, 28]. This corresponds to the observation that an antiferroelectric phase is generally stabilized under pressure [29, 30].

An important refinement of the model involves introducing the coupling of the antiferroelectric and ferroelectric order parameters to strain [31]. The addition of strain terms is generally at lowest order. A simple model incorporating hydrostatic pressure and volume change was introduced in Ref. 32 via a transformation from a Kittel model generalized to include strain:

$$G_1 = \frac{1}{2}\alpha P_F^2 + P_A^2 + \frac{\beta}{8}(P_F^4 + 6P_A^2P_F^2 + P_A^4) + \frac{\gamma}{24}(P_F^6 + 15P_A^4P_F^2 + 15P \quad (3)$$

where p is the hydrostatic pressure and Q and Ω are electrostrictive coefficients. Choice of $\beta < 0$, $\gamma > 0$ and $\eta > 0$ gives a first-order antiferroelectric transition. α is the only temperature-dependent parameter, with an assumed linear dependence $\frac{d\alpha}{dT} = \frac{1}{\epsilon_0 C}$ where ϵ_0 is the permittivity of free space and C is the Curie-Weiss constant. Analysis of the model shows that the antiferroelectric transition temperature $T_N(p)$ depends on pressure according to $T_N(p) = T_N - 2Q\epsilon_0 C(1 - \Omega)p$. If $\Omega < 0$, there is the possibility of a antiferroelectric-to-ferroelectric phase transition with increasing pressure at a critical pressure $(\eta/2Q)|\Omega|$; conversely, if $\Omega > 0$, a material can be driven from a ferroelectric to an antiferroelectric phase with applied pressure. In the latter case, a poled ferroelectric ceramic releases all polarization charges and can supply very high instantaneous current [33]. Finally, the volume change and entropy change at the antiferroelectric-paraelectric transition are related to the sublattice polarization P_A by $\Delta V/V = Q(1 - \Omega)P_A^2$ and $\Delta S = (1/2\epsilon_0 C)P_A^2$. By fitting to experimental data, the Q value for $PbZrO_3$ ($2.03 \times 10^{-2} m^4 C^{-2}$) was found to be similar to that of perovskite ferroelectrics such as $BaTiO_3$ and $PbTiO_3$, while that for $Pb(Mg_{1/2}W_{1/2})O_3$ is several times larger; the difference was associated with

the degree of cation disorder.

Models are valuable for a unified description of the properties of antiferroelectrics. They are also useful for the study of individual materials, such as $PbZrO_3$, for which a detailed phenomenological model has been obtained [34], and can be used as well to predict the behavior of epitaxially strained thin films and thin layers in superlattices.

MICROSCOPIC ORIGINS OF MACROSCOPIC BEHAVIOR

The question now becomes that of identifying antiferroelectric materials and relating their macroscopic behavior to microscopic aspects of the crystal structure and energetics. To make this macroscopic-microscopic connection, we begin by considering simple microscopic models in which the degrees of freedom are reorientable localized electric dipoles on a bipartite lattice, so that the lattice sites can be divided into two sublattices, with each site being neighbored by sites in the other sublattice. Early theoretical studies [20, 35, 37] took the interactions between dipoles to be given simply by the electrostatic dipole-dipole interaction. However, it has been well established in first-principles studies of ferroelectricity that short-range interactions deviate strongly from this asymptotic form, and that the form of the short-range interactions dominates the phase energetics [38, 39]. Furthermore, a single nearest-neighbor interaction favoring antialignment is not enough to give the characteristic double-hysteresis loop with a jump in polarization from the antiferroelectric state to the field-induced ferroelectric state [40]. Next-nearest neighbor intra-sublattice interactions to stabilize sublattice polarization formation have been shown to produce a double hysteresis loop in an Ising model (fixed-length dipole with two opposite orientations) [41]. This model yields the correct stabilization of an antiferroelectric phase and a ferroelectric phase with similar energy because a substantial energy is associated with formation of the sublattice polarization, with a smaller energy associated with the difference between alignment and antialignment of the polarizations of the two sublattices.

To connect this genre of models directly to real antiferroelectric materials requires the identification of localized reorientable dipoles occupying well-defined sites in the crystal, in analogy to the case of antiferromagnets. However, isolation of dipoles on two (or more) sublattices is much less common in the case of antiferroelectrics than in antiferromagnets, in which many systems have easily identified localized spins arising from open d or f shells in constituent atoms. Indeed, this has been the subject of much attention in the investigation of ferroelectric materials, where most are not describable as a lattice of separable reorientable dipoles or polarizable entities, and definitions of the polarization incorporate not only ion positions but the quantum mechanical wavefunctions of the electrons [42, 43]. Similarly in the present case, a definition of antiferroelectrics that required localized dipoles would be too restrictive, including only hydrogen bonded antiferroelectrics (in which the dipole is created by the two positions for a hydrogen in the bond), crystals incorporating small reorientable dipolar molecules [37] and, if the requirement for crystallinity is loosened, antiferroelectric liquid crystals where the dipole is associated with a single molecule or molecular subunit.

Another approach to making the macroscopic-microscopic connection is to follow the analogy to the soft mode theory of ferroelectricity. The first step is to identify the lattice modes of definite symmetry in the structure of the antiferroelectric phase relative to a high-symmetry reference structure (generally the paraelectric phase), and then to expand the energy in symmetry invariants to obtain the energy in the form of a Landau functional [44]. A simple Kittel-type antiferroelectric would be characterized by a single lattice mode in which the ions involved are divided into two groups with equal and opposite displacements. This mode would be expected to have a wave vector at the zone boundary, doubling the unit cell; however if the high-symmetry unit cell contains an even number of symmetry-equivalent ions involved in the mode, then the antiferroelectric phase need not have an enlarged unit cell [44].

In the more general case, other types of modes can generate the structure of the antiferroelectric phase. The distortion produced by the mode might involve more than two sublattices, with either collinear or noncollinear sublattice polarizations [45, 46], the only requirement being that the net polarization is zero. The mode might have its wave vector in the interior of the Brillouin zone, and it could be commensurate or incommensurate. Moreover, as we will see in the discussion of individual ferroelectric materials below, the antiferroelectric phase can be described by a group of coupled modes [47], with a primary unstable antipolar mode accompanied by other distortions such as oxygen octahedron rotations to which coupling is symmetry-allowed, lowering the energy of the phase.

The other key ingredient for an antiferroelectric is the presence of a low-energy alternative ferroelectric phase, which we presume to be obtained as a distortion of the same high-symmetry reference structure. The latter condition promotes a small energy difference and ease of transformation between the two phases. For the simple Kittel-type antiferroelectric, this is described by including in the model the single polar mode which is obtained from the antipolar mode by reversing the polarization of one of the two sublattices. In the more general case, the ferroelectric phase is generated by a more general zone-center polar mode and may be accompanied by other modes that are observed to be present in the low-energy

alternative ferroelectric phase. The relation of this polar mode to the primary unstable antipolar mode might be more complex than simple alignment of antipolar ionic displacements. In three dimensions, there is also the possibility that the direction of the polarization of the ferroelectric phase could be different from the direction of the sublattice polarizations of the antiferroelectric phase and could depend on the direction and magnitude of the applied electric field, so the zone-center polar mode included should be more than one dimensional.

Levanyuk [48] has pointed out that the form of the Landau functional obtained for antiferroelectrics from a Kittel-type model is not specific to a antipolar phase with well-defined sublattices, but describes any system with a nonpolar structural transition. Specifically, any system with a nonpolar structural transition, described by order parameter η, will have a generic $\eta^2 P^2$ coupling that will give the double hysteresis loops and dielectric anomalies of the Kittel model which we consider to be the defining macroscopic properties of an antiferroelectric, and thus, according to Levanyuk, "the concept of an antiferroelectric state turns out to be superfluous."

However, this statement is too strong: it should not be inferred from this analysis that any system with a nonpolar structural transition should be considered an antiferroelectric. Particular values of the parameters are required to get a structural transition with an alternative ferroelectric phase at low energy, and thus to produce the characteristic behavior in accessible applied electric fields. The Kittel two-sublattice model, when mapped to the Landau form, leads to relations between the coupling coefficients that satisfy these requirements, though this is a sufficient but not necessary condition for obtaining parameters that give antiferroelectric behavior. So, we propose here to recognize that the "antipolar" character of materials to be regarded as antiferroelectrics in fact varies on a continuum. Classic Kittel two-sublattice systems lie at one extreme. Close to this extreme is the subclass of antiferroelectrics in which the antipolar and polar instabilities are clearly related: the eigenvectors transform directly one into the other with change in wavevector, or belong to the same isolated unstable phonon branch in the high-symmetry reference structure, as computed from first principles. At the other extreme are cases where the relation between the nonpolar and ferroelectric structures is weakened to the level that the two structures are merely distortions of the same high-symmetry reference structure with a small energy difference separating the ferroelectric phase from the nonpolar phase. As there is no clear demarcation point between the two extremes, we include all of these as antiferroelectrics; this is further justified as the materials at this opposite end of the spectrum still exhibit the macroscopic properties considered characteristic of antiferroelectrics.

As an application of this formulation of the definition of antiferroelectricity, we consider orthorhombic *Pnma* $GdFeO_3$-type perovskites. This structure is generated from the cubic ideal perovskite structure by an M-point oxygen octahedron rotation around [001] combined with an R-point oxygen octahedron rotation around [110]. In this space group, additional lattice modes are symmetry allowed, including a mode at the X point $\frac{\pi}{a}(001)$ which involves antipolar displacements of the A cations along the orthorhombic a direction (approximately along the primitive perovskite [110] direction); cations in the same xy plane move together and the displacements alternate from plane to plane. However, this antipolar distortion alone is not sufficient to establish the material as antiferroelectric. In the general case, these displacements are induced by the primary oxygen-octahedron rotation instabilities and cannot be aligned by an applied field, so that there is no related ferroelectric phase at low energy. A *Pnma* perovskite can be antiferroelectric in the Kittel limit if the antipolar X mode belongs to a unstable phonon branch that includes a related polar instability and is in fact the primary instability, with the oxygen octahedron rotations resulting in a relatively small further lowering of the energy. First-principles calculations of the phonon dispersion can assist in identifying a material of this type, with $BiCrO_3$, to be discussed below in Section , as a possible example [49]. With the broader definition of antiferroelectricity that we are using here, the high-symmetry reference structure need only have a zone-center instability that produces a competing ferroelectric phase at a sufficiently low energy that an electric field can drive a first order transition to this phase. In this sense, (Bi,Sm)FeO_3 satisfies this condition near the rhomobohedral-orthorhombic compositional phase boundary, with a first-order electric-field induced phase transition from the orthorhombic *Pbnm* phase to the polar *R*3*c* phase [50].

We have seen here that reexamination of the definition and of the generally accepted properties of antiferroelectrics leads to a rather inclusive definition of antiferroelectricity. The definition hinges not on a structural criterion, as almost any nonpolar distortion of a high-symmetry reference structure could satisfy the requirements, but on energetic criteria. The essential point is that the candidate antiferroelectric phase be close in energy to a competing ferroelectric phase, to which it can be driven by an applied electric field through a first order transition. This criterion can be evaluated in several ways. If the candidate antiferroelectric phase is generated by a single antipolar mode with a clear relation to a zone center polar mode, it can be inferred that the zone center polar mode will also be unstable and generate the necessary competing ferroelectric phase. The presence of a low energy competing ferroelectric can also be inferred from proximity, across a first-order phase boundary, of the candidate antiferroelectric phase to ferroelectric phases in the generalized phase diagram for the system which includes control parameters such as

pressure, epitaxial strain and compositional substitution. First principles calculations can be used to establish the relation between antipolar and zone center polar instabilities and the low energy of a competing ferroelectric phase. In the end, direct experimental observation of an electric field induced transition to a ferroelectric phase is the most definitive indication of antiferroelectricity. In general, even if the phase satisfies this energetic criterion even for some range of control parameters, the entire phase will be referred to as antiferroelectric; this corresponds to the analogous case for ferroelectrics, in which a phase is referred to as ferroelectric even if it is not switchable by applied fields throughout its region of stability in the phase diagram.

ANTIFERROELECTRIC MATERIALS: STRUCTURE AND PROPERTIES

In this section, we consider the structure and properties of individual antiferroelectric materials as determined from experimental observation and theoretical analysis. The main focus will be on $PbZrO_3$ and related systems; two excellent recent reviews [15, 17] provide additional details and references. Other well-established antiferroelectric materials include certain niobate perovskites, vanadates and complex perovskite oxides; in each of these cases we will consider the extent to which the system satisfies the structural and energetic criteria for antiferroelectricity. The possibility of antiferroelectricity has also been raised for a number of additional systems, and the evidence relating to these systems will be discussed.

$PbZrO_3$ is, by far, the most thoroughly studied antiferroelectric oxide. Ref. 15 provides a recent detailed review; here, we highlight the most relevant aspects of the structure and properties. At high temperatures, $PbZrO_3$ has a paraelectric cubic ideal perovskite structure, and at temperatures below $T_c = 505$ K, the structure is an antiferroelectric orthorhombic distorted perovskite structure [10]. In a very narrow temperature range separating these two phases, an intermediate ferroelectric rhombohedral phase with polarization along [111] has been reported in some studies [51].

The details of the structure of the antiferroelectric phase were controversial for some time, with even the space group assignment differing between nonpolar orthorhombic *Pbam* and polar orthorhombic *Pba*2. The main features of the structure can be described in terms of modes of the primitive perovskite structure. In addition to the Σ_2 mode [52] at $q = \frac{2\pi}{a}(1/4,1/4,0)$, producing an antipolar arrangement with shifts of the lead ions along [110], shown in Figure 3, the other dominant distortion in the structure is an oxygen octahedron rotation mode R_5^- with rotation around [110]. Symmetry analysis shows that these two modes generate the space group

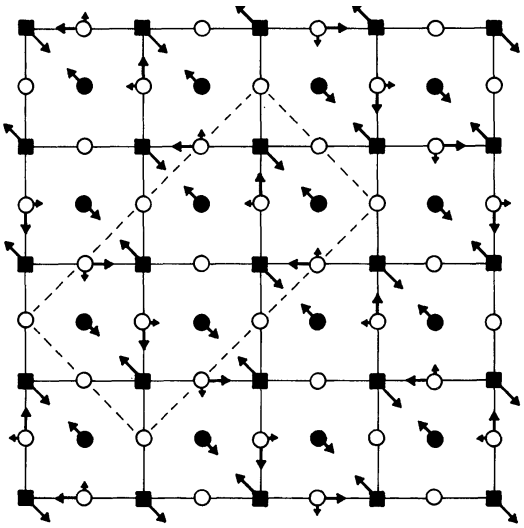

FIG. 3: Projection of atomic displacements associated with the Σ_2 mode at $q = \frac{2\pi}{a}(1/4,1/4,0)$ onto the ab plane. Squares and circles indicate Pb and oxygen atoms, respectively. Filled and open circles show atoms on the Pb atomic layer and atoms on the Zr atomic layer, respectively. From Ref. [53].

Pbam with a $\sqrt{2}a_0 \times 2\sqrt{2}a_0 \times 2a_0$ unit cell (8 formula units), as shown in Figure 4, In this structure, additional modes R_4^-, M_5^-, X_1^+ and a mode with $q=\frac{2\pi}{a}(1/4,1/4,1/2)$ are allowed without breaking further symmetry. These are found to be relatively small, and indeed are set to zero in some structure determinations to reduce the number of free parameters in the refinement (see, for example, Ref. 54). It has been suggested that the structure also includes a small zone-center polar distortion, putting it into the *Pba*2 space group [55]. First principles calculations [56–58] played a critical role in resolving this ambiguity in favor of the nonpolar *Pbam* structure. These calculations showed that optimized positions of the O atoms in the *Pbam* structure were in good agreement with available experiments, including subsequent determinations [54]. In the initial study [56], the energy of the antiferroelectric *Pbam* structure was found to be slightly lower (20 meV/f.u.) than that of the optimized rhombohedral *R*3*m* ferroelectric structure; in Ref. 58, this comparison was extended to the *Pbam* structure with full optimization of oxygen positions and the rhombohedral *R*3*c* ferroelectric structure observed to be stable with 7% Ti substitution [59], with the antiferroelectric structure found to be 31 meV/f.u. lower. This small energy difference is a key signature of an antiferroelectric material and is also consistent with the transformation to the rhombohedral FE phase at small Ti doping.

As shown in Figure 2, double hysteresis loops were observed in the earliest work on $PbZrO_3$, identifying it as an antiferroelectric [10]. The critical field is rather high, and can be lowered by doping as discussed below. The change in volume at the field-induced transition is rela-

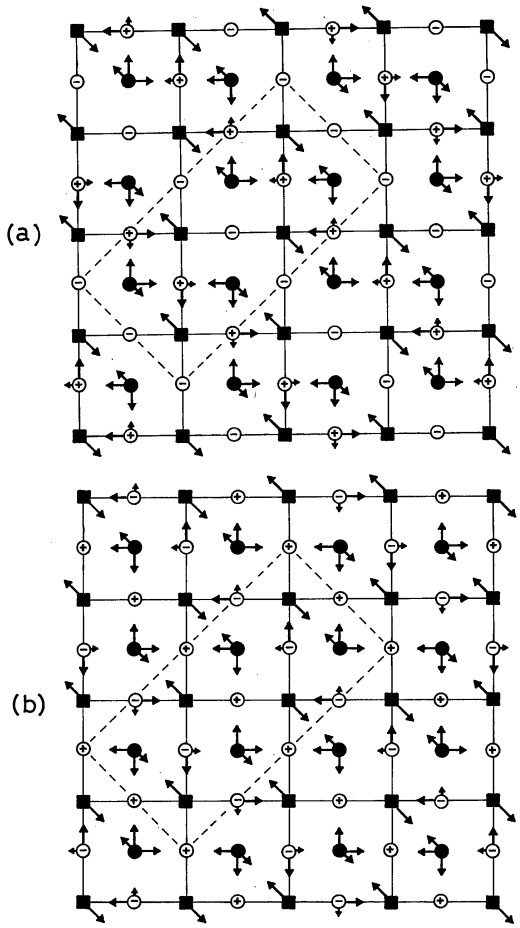

FIG. 4: Projection of atomic displacements associated with the Σ_2 and R_5^- modes onto the ab plane. Squares and circles indication Pb and oxygen atoms, respectively. Filled and open circles show atoms on the Pb atomic layer and atoms on the Zr atomic layer, respectively. Part (a) shows atoms in the planes $z = 0$ and $z = 1/2c_p$ (open symbols) and part (b) shows atoms in the planes $z = c_p$ and $z = 3/2c_p$ (open symbols) where c_p is the pseudocubic lattice parameter in the z direction. From Ref. [53].

tively large, which is favorable for strain-related properties but may reduce the reversibility of the transition. A more detailed discussion of the field-induced ferroelectric phase can be found in Ref. 60.

Given that the antiferroelectric phase of $PbZrO_3$ is not described by two oppositely-polarized sublattices, and the additional complication of the intermediate ferroelectric phase, it should be asked to what degree $PbZrO_3$ behaves according to the models described above. Analysis of the amplitudes of Pb displacements, oxygen octahedron rotations and lattice strains as a function of temperature are reported to be well described by a simple Landau theory for a first-order transition out of the antiferroelectric phase [61]. This theory was developed in more detail in Ref. 34 to describe the dielectric response and elastic properties. In these theories, the antiferroelectric distortion is described by an order parameter that does not specifically require a two-sublattice character for the distortion.

The compositional-substitution phase diagrams of $PbZrO_3$ provide further evidence of its antiferroelectric character. The fact that in many cases, a small fraction of compositional substitution induces a first-order transition to a ferroelectric phase confirms that there is an alternative ferroelectric phase at low energy in pure $PbZrO_3$. By lowering the energy difference in favor of the ferroelectric phase, these substitutions also lower the critical field for the electric-field induced transition [63]. Some examples include $Pb_{1-x}Ba_xZrO_3$ [64] in which Ba substitution reduces the relative free energy of the ferroelecric phase, thus lowering the critical field, and widening the range of stability of the intermediate ferroelectric phase. This system illustrates the challenge that compositional tuning to improve one materials property (here, the critical field) may worsen others: in Ref. 62 it is shown that $Pb_{1-x}Ba_xZrO_3$ exhibits temperature irreversibility (that is, the antiferroelectric phase is not recovered from the ferroelectric phase on cooling) and other references with similar observations are discussed. The tuning of critical electric field, structural parameters, and associated properties such as reversibility of the transitions has prompted extensive experimentation with complex substitutions, such as $Pb_{0.89}Nb_{0.02}[(Zr_{0.57}Sn_{0.43})_{0.94}Ti_{0.06}]_{0.98}O_3$ (also referred to as PNZST43/100y/2) [26, 65–68].

Study of compositional substitution phase diagrams also suggests that there are low-energy alternative antiferroelectric phases of distinct structure as well; this was noted already in the early work by Shirane [11]. Substitution of Pb by Sr is shown to result in an antiferroelectric intermediate phase separating the high-temperature paraelectric phase from the low-temperature $PbZrO_3$-like antiferroelectric phase [11]. In $PbZr_{1-x}Sn_xO_3$, a distinct antiferroelectric $P222_1$ phase is observed for x $>$ 0.05; only for x $>$ 0.3 does an $R3m$ ferroelectric phase become stable [69].

$PbHfO_3$ was first reported as antiferroelectric soon after the identification of antiferroelectricity in $PbZrO_3$ [70]. Despite their chemical similarity, the phase sequence is different from that of $PbZrO_3$ [71–73]: phase I (up to 163 C) is tetragonal with c/a $<$ 1, phase II (163-215 C) is tetragonal with a larger c/a (still less than 1) and phase III (above 215 C) is cubic. Phases I and II have both been characterized as antiferroelectric. Phase I appears to be isomorphic to the orthorhombic AFE structure of PZ. Less is known about Phase II. It appears to have a very large unit cell [72] and to be nonpolar, consistent with Raman scattering observations [74], and it has been suggested that it should be assigned to one of the orthorhombic space groups $P222_1$, $Pmm2$, $Pmmm$ or $P222$ [75, 76].

$NaNbO_3$ and $AgNbO_3$ are perovskite systems which

both show antiferroelectric phases as part of a complex sequence of phases with temperature [77–80]. The room temperature antiferroelectric phases in the two materials are isostructural in orthorhombic space group *Pbcm* with eight formula units per $\sqrt{2}a_0 \times \sqrt{2}a_0 \times 4a_0$ unit cell. The structure is characterized by oxygen octahedron rotations as well as a $\vec{q}$=(0,0,π/2) mode, involving antipolar Nb displacements, that is responsible for the designation as an antiferroelectric [79]. In $NaNbO_3$, there is a transition to a low-temperature ferroelectric *R3c* phase at 173 K and a sequence of phase transitions starting at 633 K and ending with a transition to a cubic paraelectric phase at 913 K [81]. In $AgNbO_3$, the room temperature antiferroelectric phase appears stable down to low temperature, and there is a different transition sequence with increasing temperature: two transitions have been tentatively identified at 340 K and 540 K but without any apparent change in symmetry, and starting at 626 K there is a sequence of phase transitions through orthorhombic and tetragonal phases that ends with a transition to a cubic paraelectric phase at 852 K [81]. First principles calculations have focused mainly on the zone center polar modes and oxygen octahedron rotations [82–87]. The lattice instabilities of the cubic perovskite structure are identified for $AgNbO_3$ and $NaNbO_3$. Both show unstable modes for oxygen octahedron rotations at R and M, as well as a unstable ferroelectric mode. This can produce a set of competing low energy states consistent with the observed sequence of phases. The electric field induced transition to a ferroelectric phase in $NaNbO_3$ has been well studied [88–90]; and occurs at high field perpendicular to the orthorhombic c axis. The dependence of the transition on the direction of the field has been studied in detail; a clear distinction can be drawn between transitions in which the polarization of the ferroelectric phase is along essentially the same direction as the sublattice polarizations of the antiferroelectric phase, and those in which it is along a different direction [90]. In addition, a small amount of K substitution for Na produces a ferroelectric phase at room temperature [91].

While, as discussed above, the orthorhombic *Pnma* perovskites are generally not antiferroelectric, there can be some exceptions to this rule. The clearest would be in cases where the local dipolar distortions are driven by the A-site Pb or Bi displacements. The first-principles phonon dispersion for $BiCrO_3$ shows a clear antipolar instability at the X point related to a polar instability at Γ, and characteristic antiferroelectric hysteresis loops have been observed in films [92]. However, it should be noted that the measurements were made for a lower symmetry phase, not the *Pbnm* phase. $BiFeO_3$ is a ferroelectric, but with RE doping on the Bi site, undergoes a transition to an orthorhombic *Pbnm* phase. In this phase near the critical doping, double hysteresis loops are observed with the electric field inducing a transition back to the polar *R3c* ferroelectric phase [50]. With our inclusive definition of antiferroelectricity, the doped system (and even pure $SmFeO_3$, since it is the same phase) can be considered antiferroelectric. Other nonpolar Bi perovskites, such as $BiMnO_3$, might also be antiferroelectric given proximity to a ferroelectric phase; indeed $BiMnO_3$ was thought for a while to be ferroelectric before additional experiments and first-principles calculations established that the ground state structure is nonpolar [93, 94]. Antiferroelectricity has also been discussed for $Sr_{1-x}Ca_xTiO_3$ [95].

Antiferroelectric phases have also been identified in double perovskites. The degree of cation disorder is a key feature in characterizing double perovskite systems. Cation disorder generally yields relaxor behavior, while a number of well-ordered systems show phases isostructural to $PbZrO_3$, which are thus characterized as antiferroelectric. A theoretical analysis is given in Ref. 96. One example is $Pb(In_{1/2}Nb_{1/2})O_3$ [97–99] which is seen to have an antiferroelectric phase isostructural with $PbZrO_3$. Study of the $PbNb_{1/2}B_{1/2}O_3$ series [100] shows a transition from ferroelectric (B = Cr, Fe, Mn, Sc, In) to nonpolar (B = Lu, Yb, Tm) low-temperature phases depending on the B ionic radius; the case of B = In is at the crossover and thus the close competition between ferroelectric and nonpolar phases characteristic of antiferroelectricity is expected. A phase sequence from paraelectric to antiferroelectric to low temperature ferroelectric has been identified for a number of lead-based double perovskite systems including $Pb(Yb_{1/2}Nb_{1/2})O_3$ [101], PYN-PT [102], $Pb(Yb_{1/2}Ta_{1/2})O_3$ [103], $Pb(Co_{1/2}W_{1/2})O_3$ [104] and $Pb(Sc_{1/2}Ta_{1/2})O_3$ [104, 105]. No detailed structural determination has been made of the antiferroelectric phases. Additional observations of antiferroelectric phases have been reported for non-lead perovskites, including $Na(Bi_{1/2}Ti_{1/2})O_3$ [106], $Bi(Mg_{1/2}Ti_{1/2})O_3$ (BMT) [107] and BNT-BT [108]. More information and references about these systems can be found in Ref. [17].

Antiferroelectricity has been noted in a number of other compounds, including $NaVO_3$ (mentioned in Ref. 109) and WO_3 [110]. $BiNbO_4$ is found to be paraelectric above 570 C, ferroelectric between 360 and 570 C and nonpolar below 360 C [111]. The latter phase can be presumed to be antiferroelectric due to its proximity to the intermediate ferroelectric phase. A dielectric anomaly observed at the Jahn-Teller transition of $DyVO_4$ (T_c = 15.2 K) was attributed to a strain-induced staggered polarization on two sublattices within the zircon unit cell [112]. The electric field needed to produce alignment of the two sublattices was estimated from a model analysis to be two orders of magnitude greater than that for $PbZrO_3$. To the extent that this meets the energetic criterion for antiferroelectricity, $DyVO_4$ would be a rare example of a antiferroelectric in which the unit cell does not change in the paraelectric-antiferroelectric transition. Finally, some exotic examples include early reports of antiferroelectricity in spinels [**?**],betaine phosphate [114],

hydroyapatite, and thiourea, and more recently, in hybrid organic-inorganic metal-organic-framework (MOF) structures [115].

RELATION TO ALTERNATIVE FERROELECTRIC PHASES

As previously noted, none of the known antiferroelectric compounds conform to the collinear two-sublattice Kittel model. Therefore, in all known compounds, the electric-field-induced ferroelectric phase is not obtained from the antiferroelectric structure simply by flipping one of the sublattice polarizations. Even in a hypothetical Kittel-type compound, application of an electric field noncollinear with the sublattice polarization could lead to a nontrivial induced phase. The relation between the structure of the antiferroelectric phase and the structure of the alternative ferroelectric phases induced by electric fields or by changes in control parameters such as compositional substitution and epitaxial strain is therefore of considerable interest.

First principles studies of the electric field induced transitions for noncollinear fields (polarization rotation) have proved illuminating for ferroelectrics [116–118]. Modeling of electric field induced transitions in antiferroelectrics include studies of $PbZrO_3$ and $NaNbO_3$ [90].

ANTIFERROELECTRICITY IN THIN FILMS

The behavior of materials in thin film form is modified by strain, size effects, and structural and electronic relaxation and reconstruction at the surfaces and interfaces. These factors can strongly affect the energy difference between the antipolar and polar phases. In particular, an antiferroelectric material, in which this energy difference is small, can in some cases be tuned to the phase boundary with the related ferroelectric phase. Similarly, a bulk ferroelectric material with a low-energy alternative antipolar phase (which may not be manifest in observations of the bulk) could be driven antiferroelectric in thin film form; in both cases the depolarization field associated with any uncompensated polarization along the normal would tend to suppress the formation of a single-domain ferroelectric film. This tuning needs to be taken into consideration in the application of these materials in thin film devices: it can be beneficial as well as detrimental that the material in thin film form behaves differently from the material in bulk.

Thin films of $PbZrO_3$ have received the most attention. The electric-field-induced transition in a film on a Pt-coated Si substrate was reported to occur at 140 kV/cm for increasing field and 71 kV/cm for decreasing field, with a maximum polarization of 40 $\mu C/cm^2$ [119]. In another study, thin films of $PbZrO_3$ were grown on crystalline Si(100) with thicknesses ranging from 100 nm to 900 nm. At thicknesses below 500 nm, ferroelectric hysteresis loops were observed with spontaneous polarization of 31 $\mu C/cm^2$ and coercive field of 100 kV/cm at thickness of 260 nm; similar behavior was observed for thin films of antiferroelectric $BiNbO_4$ [120]. The appearance of ferroelectricity was attributed in this work to the electric field produced at the interface, rather than strain or size effects, because an earlier experiment reported double hysteresis loops in a 380 nm-thick film of $PbZrO_3$ on a Pt-coated Si substrate [121]. In contrast, in $PbZrO_3$ grown on $SrTiO_3$ with an $SrRuO_3$ buffer layer, corresponding to over 5% compressive strain, 8 nm thick films showed a ferroelectric rhombohedral phase with a high density of misfit dislocations, while thicker films showed the rhombohedral phase for the first 8 nm and then a bulk-like orthorhombic phase; this was attributed to the higher strain near the interface [16].

FIG. 5: Schematic hysteresis loops for ferroelectrics, relax or ferroelectrics and antiferroelectrics. The shaded area corresponds to the stored energy density. From Ref. [131].

Superlattices of antiferroelectrics with ferroelectrics can show rich behavior due to the competition between the two phases. In single-unit-cell layers, it can be argued that the antiferroelectric phase cannot develop fully, and alternative structures are stabilized [122]. In thicker layers, the behavior evolves in a systematic way [123].

PROPERTIES FOR APPLICATIONS

There has been increasing interest in the technological applications of antiferroelectric materials [16]. Proposed applications include sensors, actuators, energy and charge storage devices, voltage regulators and electro-optic devices [124–129].

The relevance to energy storage applications comes from the enhancement of DdE by the shape of the double hysteresis loop (see Figure 5). The energy stored is roughly twice what is stored by a linear dielectric with the same polarization at a field just above the transition field. Patented devices include a cardiac defibrillator [130].

The strain change at the electric-field induced transition has received particular attention, with proposals of strain and force generators [132] and electrostrictors with high strain response and small temperature dependence of strain [108]. In an applied electric field, the

strain difference between the antiferroelectric and ferroelectric phases can result in a large nonlinear response. Specifically, the electric-field induced transition from the antiferroelectric to the ferroelectric phase, with a large jump in electrical polarization as seen in the double hysteresis loop, can be accompanied by a large strain change (in $PbZrO_3$, a volume expansion). Observations in $(Pb_{0.97}La_{0.02})(Sn,Ti,Zr)O_3$ (PLZT) [33] and lead-free perovskites [133] suggest the application of this behavior for large-strain actuators. In PLZT it is observed that the field-induced polarization is almost temperature independent while the field-induced strain depends strongly on temperature. An intriguing twist has been noted in Ref. 26. In a system in which applied pressure drives a transition from the ferroelectric phase to an antiferroelectric phase, the decrease in volume of a poled ferroelectric ceramic when a reversed polarity electric field is applied can induce a transition into the antiferroelectric phase, with the counterintuitive effect that an electric field drives a system from ferroelectric to antiferroelectric.

PROSPECTS

This reexamination of antiferroelectricity in oxides raises many questions. Antiferroelectric materials overall have received much less attention than ferroelectrics, and only a few materials have been thoroughly studied. Much of the work has been on compositional tuning of $PbZrO_3$ and the lead-free perovskites to control essential features such as transition temperature, critical field, strain response and reversibility of the electric-field-induced transition, leading to complex multi-component systems. On the other hand, many nonpolar phases have been given the designation antiferroelectric without verification of the energetic criterion of a distinct low-energy ferroelectric phase.

A systematic approach to design and discovery of new antiferroelectric materials is therefore indicated. For example, it is striking that there is no oxide antiferroelectric that conforms to the simple two-sublattice Kittel model. Also, it would be a curiosity to find a definitive example of an antiferroelectric driven by a $q = 0$ lattice. Though the perovskite structure could in principle support such a phase, driven by the zone-center silent mode in which two oxygens move in equal and opposite directions, no compound in this structure is reported in ICSD. A more promising route to new antiferroelectrics is to follow the paradigm set by the canonical antiferroelectric oxide $PbZrO_3$. As we have seen above, the antipolar structure of $PbZrO_3$, is generated by a non-zone-boundary phonon, with auxiliary oxygen-octahedron rotation distortions stabilizing the antiferroelectric phase; a number of perovskite systems have been shown to have this same structure. It it possible that the reason this particular structure appears so prevalent is that, given the familiarity of $PbZrO_3$, it is easy to recognize. In fact, it would seem that there should be other, perhaps many choices, for antipolar phonons that could yield low energy structures when coupled to other modes. First principles calculations of full phonon dispersion of high-symmetry reference structures, including but not limited to perovskites, can be very valuable in identifying such instabilities and structures. Another promising approach, based on combination of high-throughput first-principles calculations with crystallographic database mining, is described in Ref. 134.

The functional properties of antiferroelectrics arise for the most part from the changes in properties of the material at the electric-field-induced transition; the most well-studied examples being the electric polarization, the strain and optical properties. As more classes of antiferroelectric materials are developed, there are opportunities to improve functional behavior by targeting particular properties for contrast in the two phases. For example, the two phases could have different magnetic ordering, leading to spin-lattice effects and magnetoelectric properties that are the subject of great current interest of multiferroics. It has already been demonstrated that antiferroelectric lattice instabilities can be favored by magnetic ordering, specifically, in perovskite $LuCrO_3$, in which the silent mode becomes unstable for the higher energy ferromagnetic ordering [135]. Yet other functionalities could be accessed by consideration of ferrielectrics, in which the sublattice polarizations of the "antiferroelectric" phase do not completely cancel, resulting in a net spontaneous polarization. These would show the characteristic behavior of antiferroelectrics at the electric-field-induced transition, but also could have a switchable polarization at lower fields [136].

In conclusion, this brief review and reexamination of the fundamental physics of antiferroelectricity suggests that these are a rich and interesting class of functional materials whose potential has yet to be fully tapped. Further study, especially in materials design, synthesis and characterization, should lead to significant progress, with the possibility of a variety of novel device technologies.

Acknowledgments

I acknowledge the support of ONR grant N00014-09-1-0302, MURI-ARO grant W911-NF-07-1-0410 and NSF MRSEC DMR-0820404. Part of the preparation of this chapter was carried out at the Aspen Center for Physics. I thank J. W. Bennett, C. J. Fennie, D. R. Hamann, K. Garrity, S. Reyes-Lillo and D. Vanderbilt for useful discussions.

[1] C. J. Fennie and K. M. Rabe, "Magnetic and electric phase control in epitaxial $EuTiO_3$ from first principles,"

Phys. Rev. Lett. 97, 267602 (2006).
[2] C. J. Fennie, "Ferroelectrically-induced weak ferromagnetism by design," Phys. Rev. Lett. 100, 167203 (2008)
[3] N. A. Benedek and C. J. Fennie, "Hybrid improper ferroelectricity: A mechanism for controllable polarization-magnetization coupling," Phys. Rev. Lett. 106, 107204 (2011).
[4] D. G. Schlom, L. Q. Chen, C. B. Eom, K. M. Rabe, S. K. Streiffer and J. M. Triscone, "Strain tuning of ferroelectric thin films," Ann. Rev. Mat. Res. 37, 589 (2007).
[5] R. Armiento, B. Kozinsky, M. Fornari and G. Ceder, "Screening for high-performance piezoelectrics using high-throughput density functional theory," Phys. Rev. B 84, 014103 (2011).
[6] X. Zhang, L. Yu, A. Zakutayev and A. Zunger, "Sorting stable versus unstable hypothetical compounds: The case of multi-functional ABX half-Heusler filled tetrahedral structures," Adv. Funct. Mat. 22, 1425 (2012).
[7] A. Roy, J. W. Bennett, K. M. Rabe and D. Vanderbilt, "Half-Heusler semiconductors as piezoelectrics," Phys. Rev. Lett. 109, 037602 (2012).
[8] J. W. Bennett, K. Garrity, K. M. Rabe and D. Vanderbilt, "Hexagonal ABC compounds as semiconducting ferroelectrics, Phys. Rev. Lett. 109, 167602 (2012).
[9] N. A. Spaldin, *Magnetic Materials: Fundamentals and Applications,* 2nd ed. (Cambridge University Press, 2010).
[10] G. Shirane, E. Sawaguchi and Y. Takagi, "Dielectric properties of lead zirconate," Phys. Rev. 84, 476 (1951).
[11] G. Shirane, "Ferroelectricity and antiferroelectricity in ceramic $PbZrO_3$ containing Ba or Sr," Phys. Rev. 86, 219 (1952).
[12] B. A. Strukov and A. P. Levanyuk, *Ferroelectric Phenomena in Crystals: Physical Foundations* (Springer-Verlag, 1998).
[13] A. S. Mischenko, Q. Zhang, J. F. Scott, R. W. Whatmore and N. D. Mathur, "Giant electrocaloric effect in thin film $PbZr_{0.95}Ti_{0.05}O_3$," Science 311, 1270 (2006).
[14] J. Parui and S. B. Krupanidhi, "Electrocaloric effect in antiferroelectric $PbZrO_3$ thin films," Phys. Stat. Sol. 2, 230 (2008).
[15] H. Liu and B. Dkhil, "A brief review on the model antiferroelectric $PbZrO_3$," J. Kristallog. 226, 163 (2011).
[16] A. R. Chaudhuri, M. Arredondo, A. Hahnel, A. Morelli, M. Becker, M. Alexe and I. Vrejoiu, "Epitaxial strain stabilization of a ferroelectric phase in $PbZrO_3$ thin films," Phys. Rev. B 84, 054112 (2011).
[17] X. Tan, C. Ma, J. Fredrick, S. Beckman and K. G. Webber, "The antiferroelectric-ferroelectric phase transition in lead-containing and lead-free perovskite ceramics," J. Am. Ceram. Soc. 94, 4091 (2011).
[18] M. E. Lines and A. M. Glass, *Principles and Applications of Ferroelectrics and Related Materials* (Cambridge University Press, 1977).
[19] T. Mitsui, "Ferroelectrics and antiferroelectrics," in *Springer Handbook of Condensed Matter and Materials Data*, part 4, pp. 903-938 (Springer-Verlag, 2005).
[20] C. Kittel, "Theory of antiferroelectric crystals," Phys. Rev. 82, 729 (1951).
[21] F. Jona and G. Shirane, *Ferroelectric Crystals* (Pergamon, 1962).
[22] L. E. Cross, "Antiferroelectric-ferroelectric switching in a simple "Kittel" antiferroelectric," J. Phys. Soc. Japan 23, 77 (1967).
[23] K. Okada, "Phenomenological theory of antiferroelectric transition. I. Second-order transition," J. Phys. Soc. Japan 27, 420 (1969).
[24] K. Okada, "Phenomenological theory of antiferroelectric transition. III. Phase diagram and bias effects of first-order transition," J. Phys. Soc. Japan 37, 1226 (1974).
[25] R. E. Cohen, "Origin of ferroelectricity in perovskite oxides," Nature 358, 136 (1992).
[26] X. Tan, J. Frederick, C. Ma, W. Jo and J. Rodel, "Can an electric field induce an antiferroelectric phase out of a ferroelectric phase?" Phys. Rev. Lett. 105, 255702 (2010).
[27] D. H. Zeuch, S. T. Montgomery and D. J. Holcomb, "Uniaxial compression experiments on lead zirconate titanate 95/5-2Nb ceramic: Evidence for an orientation-dependent, maximum compressive stress criterion for onset of the ferroelectric to antiferroelectric polymorphic transformation," J. Mater. Res. 15, 689 (2000)
[28] M. Avdeev, J. D. Jorgensen, S. Short, G. A. Samara, E. L. Venturini, P. Yang and B. Morosin, "Pressure-induced ferroelectric to antiferroelectric phase transition in $Pb_{0.99}(Zr_{0.95}Ti_{0.05})_{0.98}Nb_{0.02}O_3$," Phys. Rev. B 73, 064105 (2006).
[29] G. Samara, T. Sakudo, K. Yoshimitsu, "Important generalization concerning the role of competing forces in displacive phase transitions," Phys. Rev. Lett. 35, 1767 (1975).
[30] P. Yang and D. A. Payne, "The effect of external field symmetry on the antiferroelectric-ferroelectric phase transformation," Journal of Applied Physics 80, 4001 (1996).
[31] W. P. Mason, "Properties of a tetragonal antiferroelectric crystal, Phys. Rev. 88, 480 (1952).
[32] K. Uchino, L. E. Cross and R. E. Newnham, "Electrostrictive effects in antiferroelectric perovskites," J. Appl. Phys. 52, 1455 (1981).
[33] W. Y. Pan, C. Q. Dam, Q. M. Zhang and L. E. Cross, "Large displacement transducers based on electric field forced phase transitions in the tetragonal $(Pb_{0.97}La_{0.02})$ (Ti,Zr,Sn)O_3 family of ceramics," J. Appl. Phys. 66, 6014 (1989).
[34] M. J. Haun, T. J. Harvin, M. T. Lanagen, Z. Q. Zhuang, S. J. Jang and L. E. Cross, "Thermodynamic theory of $PbZrO_3$," J. Appl. Phys. 65, 3173 (1989).
[35] M. H. Cohen, "Ferroelectricity versus antiferroelectricity in barium titanate," Phys. Rev. ?? 369 (1952).
[36] K. Uchino, S. Nomura, L. E. Cross, R. E. Newnham and S. J. Jang, "Electrostrictive effect in perovskites and its transducer applications," J. Mat. Sci. 16, 569 (1981).
[37] Y. Takagi, "Ferroelectricity and antiferroelectricity of a crystal containing rotatable polar molecules, Phys. Rev. 85, 315 (1952).
[38] W. Zhong, D. Vanderbilt and K. M. Rabe, "First-principles theory of ferroelectric phase transitions for perovskite: The case of $BaTiO_3$," Phys. Rev. B 52, 6301 (1995).
[39] U. V. Waghmare and K. M. Rabe, "Ab initio statistical mechanics of the ferroelectric phase transition in $PbTiO_3$," Phys. Rev. B 55, 6161 (1997).
[40] S. Reyes-Lillo and K. M. Rabe, unpublished.
[41] I. B. Misirlioglu, L. Pintilie, K. Boldyreva, M. Alexe and D. Hesse, "Antiferroelectric hysteresis loops with two exchange constants using the two dimensional Ising

model," Appl. Phys. Lett. 91, 202905 (2007).
[42] R. D. King-Smith and D. Vanderbilt, "Theory of polarization of crystalline solids," Phys. Rev. B 47, 1651 (1993).
[43] R. Resta, "Macroscopic polarization in crystalline dielectrics: the geometric phase approach," Rev. Mod. Phys. 66, 899 (1994).
[44] R. Blinc and B. Zeks, *Soft modes in ferroelectrics and antiferroelectrics* (North-Holland, 1974).
[45] L. A. Shuvalov and A. S. Sonin, Sov. Phys. Cryst. 6, 258 (1961).
[46] R. A. Hatt and W. Cao, "Landau-Ginzburg model for antiferroelectric phase transitions based on microscopic symmetry," Phys. Rev. B 62, 818 (2000).
[47] U. V. Waghmare and K. M. Rabe, "Lattice instabilities, anharmonicity and phase transitions in $PbZrO_3$ from first principles," Ferroelectrics 194, 135 (1997).
[48] A. P. Levanyuk and D. G. Sannikov, "Anomalies in dielectric properties in phase transitions," Sov. Phys. JETP 28, 134 (1968).
[49] N. A. Hill, P. Battig and C. Daul, "First principles search for multiferroism in $BiCrO_3$," J. Phys. Chem. B 106, 3383 (2002)
[50] D. Kan, L. Palova, V. Anbusathaiah, C. J. Cheng, S. Fujino, V. Nagarajan, K. M. Rabe and I. Takeuchi, "Universal behavior and electric-field-induced structural transition in rare-earth-substituted $BiFeO_3$," Adv. Funct. Mat. 20, 1108 (2010).
[51] K. Roleder, G. E. Kugel, J. Handerek, M. D. Fontana, C. Carabatos, M. Hafin and A. Kania, "The first evidence of two phase transitions in $PbZrO_3$ crystals derived from simultaneous Raman and dielectric measurements," Ferroelectrics 80, 161 (1988).
[52] H. T. Stokes, E. H. Kisi, D. M. Hatch and C. J. Howard, "Group theoretical analysis of octahedral tilting in ferroelectric perovskites," Acta Cryst. B 58, 934 (2002).
[53] H. Fujishita and S. Hoshino, "A study of structural phase transitions in antiferroelectric $PbZrO_3$ by neutron diffraction," J. Phys. Soc. Jpn. 53, 226 (1984).
[54] H. Fujishita and S. Katano, "Reexamination of the antiferroelectric structure of $PbZrO_3$," J. Phys. Soc. Jpn. 66, 3484 (1997).
[55] F. Jona, G. Shirane, F. Mazzi, and R. Pepinsky, "X-ray and neutron diffraction study of antiferroelectric lead zirconate, $PbZrO_3$," Phys. Rev. 105, 849 (1957).
[56] D. J. Singh, "Structure and energetic of antiferroelectric $PbZrO_3$," Phys. Rev. B 52, 12559 (1995).
[57] M. D. Johannes and D. J. Singh, "Crystal structure and electric field gradients of $PbZrO_3$ from density functional calculations," Phys. Rev. B 71, 212101 (2005).
[58] R. Kagimura and D. J. Singh, "First-principles investigation of elastic properties and energetics of antiferroelectric and ferroelectric phases of $PbZrO_3$," Phys. Rev. B 77, 104113 (2008).
[59] D. L. Corker, A. M. Glazer, R. W. Whatmore, A. Stallard and F. Fauth, "A neutron diffraction investigation into the rhombohedral phases of the perovskite series $PbZr_{1-x}Ti_xO_3$," J. Phys. Cond. Matt. 10, 6251 (1998).
[60] A. V. Leyderman, I. N. Leontev, O. E. Fesenko and N. G. Leontev, "Dipole order and stability of the ferroelectric and antiferroelectric states in lead zirconate," Phys. Solid State 40, 1204 (1998).
[61] R. W. Whatmore and A. M. Glazer, "Structural phase transitions in lead zirconate," J. Phys. C 12, 1505 (1979).
[62] B. P. Pokharei and D. Pandey, "Irreversibility of the antiferroelectric to ferroelectric phase transition in $Pb_{0.90}Ba_{0.10}ZrO_3$ ceramics," J. Appl. Phys. 86, 3327 (1999).
[63] I. Jankowska-Sumara, "Calorimetric study and Landau analysis of the phase transitions in $PbZr_{1-x}Sn_xO_3$ single crystals with $0 \leq x \leq 4$," phys. stat. sol. (b) 244, 1887 (2007).
[64] K. H. Yoon, S. C. Hwang and D. H. Kang, "Dielectric and field-induced strain behavior of $(Pb_{1-x}Ba_x)ZrO_3$ ceramics," J. Mat. Sci. 32, 17 (1997).
[65] D. Viehland, D. Forst, Z. Xu and J. F. Li, "Incommensurately modulated polar structures in antiferroelectric Sn-modified lead zirconate titanate: The modulated structure and its influences on electrically induced polarizations and strains," J. Amer. Cer. Soc. 78, 2101 (1995).
[66] X. Tan, W. Jo, T. Granzow, J. Frederick, E. Aulbach and Rdel, "Auxetic behavior under electrical loads in an induced ferroelectric phase," Appl. Phys. Lett. 94, 042909 (2009).
[67] H. He and X. Tan, "Raman spectroscopy study of the phase transitions in $Pb_{0.99}Nb_{0.02}[(Zr_{0.57}Sn_{0.43})_{1-y}Ti_y]_{0.98}O_3$ ceramics," J. Phys. Cond. Matt. 19, 136003 (2007).
[68] X. Tan, J. Fredrick, C. Ma, E. Aulbach, M. Marsilius, W. Hong, T. Granzow, W. Jo and J. Rodel, "Electric-field-induced antiferroelectric to ferroelectric phase transition in mechanically confined $Pb_{0.99}Nb_{0.02}[(Zr_{0.57}Sn_{0.43})_{0.94}Ti_{0.06}]_{0.98}O_3$," Phys. Rev. B 81, 014103 (2010).
[69] I. Jankowska-Sumara, "Phase transitions in $PbZr_{1-x}Sn_xO_3$ single crystals," Ferroelectrics 313, 81 (2004)
[70] G. Shirane and R. Pepinsky, "Phase transitions in antiferroelectric $PbHfO_3$," Phys. Rev. 91, 812 (1953).
[71] V. Madigou, J. L. Baudour, F. Bouree, Cl. Favotto, M. Rubin and G. Nihoul, "Crystallographic structure of lead hafnate ($PbHfO_3$) from neutron powder diffraction and electron microscopy," Phil. Mag. A 79, 847 (1999).
[72] H. Fujishita et al., "A study of structures and order parameters in antiferroelectric $PbHfO_3$ by synchrotron radiation," J. Phys. Soc. Jpn. 74, 2743 (2005).
[73] H. Fujishita et al., "A study of structures and order parameters in antiferroelectric $PbHfO_3$ using neutron diffraction," J. Phys. Soc. Jpn. 77, 064601 (2008).
[74] I. Jankowska-Sumara, G. E. Kugel, K. Roleder and J. Dec, "Raman scattering in pure and Ti-doped $PbHfO_3$ antiferroelectric crystals," J. Phys. Cond. Matt. 7, 3957 (1995).
[75] S. M. Zaitsev, G. P. Zhavoronko, A. A. Tatarenko, M. F. Kuprianow, V. S. Filipiev and G. E. Fesenko, Kristallografica 24, 826 (1979).
[76] N. G. Leontiev, R. V. Kolesova, V. V. Eremkin, O. E. Fesenko and V. G. Smotriakow, Sov. Phys. Crystallogr. 29, 238 (1984).
[77] A. C. Sakowski-Cowley, K. Lukaszewicz and H. D. Megaw, "The structure of sodium niobate at room temperature, and the problem of reliability in pseudosymmetric structures," Acta. Cryst. B 25, 851 (1969).
[78] C. N. W. Darlington and K. S. Knight, "High-temperature phases of $NaNbO_3$ and $NaTaO_3$," Acta Cryst. B55, 24 (1999)

[79] Ph. Sciau, A. Kania, B. Dkhil, E. Suard and A. Ratuszna, "Structural investigation of $AgNbO_3$ phases using x-ray and neutron diffraction," J. Phys. Cond. Matt. 16, 2795 (2004).

[80] S. K. Mishra, N. Choudhury, S. L. Chaplot, P. S. R. Krishna and R. Mittal, "Competing antiferroelectric and ferroelectric interactions in $NaNbO_3$: Neutron diffraction and theoretical studies," Phys. Rev. B 76, 024110 (2007).

[81] A. Kania and J. Kwapulinski, "$Ag_{1-x}Na_xNbO_3$ (ANN) solid solutions: from disordered antiferroelectric $AgNbO_3$ to normal antiferroelectric $NaNbO_3$," J. Phys. Cond. Matt. 11, 8933 (1999).

[82] R. D. King-Smith and David Vanderbilt, "First principles investigation of ferroelectricity in perovskite compounds," Phys. Rev. B 49,, 5828 (1994).

[83] W. Zhong, R. D. King-Smith and D. Vanderbilt, "Giant LO-TO splittings in perovskite ferroelectrics," Phys. Rev. Lett. 72, 3618 (1994).

[84] W. Zhong and D. Vanderbilt, "Competing structural instabilities in cubic perovskites," Phys. Rev. Lett. 74, 2587 (1995)

[85] D. Vanderbilt and W. Zhong, "First-principles theory of structural phase transitions for perovskites: Competing instabilities," Ferroelectrics 181, 206 (1998).

[86] O. Dieguez, K. M. Rabe and D. Vanderbilt, "First-principles study of epitaxial strain in perovskites," Phys. Rev. B 72, 144101 (2005)

[87] S. A. Prosandeev, "Comparative analysis of the phonon modes in $AgNbO_3$ and $NaNbO_3$," Phys. Sol. State. 47, 2130 (2005).

[88] L. E. Cross and B. J. Nicholson, "The optical and electrical properties of single crystals of sodium niobate," Phil. Mag. 46, 212 (1955).

[89] L. E. Cross, Phil. Mag. 1, 76 (1956).

[90] A. V. Ulinzheev, A. V. Leiderman, V. G. Smotrakov, V. Yu. Topolov and O. E. Fesenko, "Phase transitions induced in $NaNbO_3$ crystals by varying the direction of an external field," Phys. Sol. St. 39, 972 (1997).

[91] L. E. Cross, "Electric double hysteresis in ($K_xNa_{1-x}NbO_3$ single crystals," Nature 181, 178 (1958).

[92] D. H. Kim, H. N. Lee, M. Varela and H. M. Christen, "Antiferroelectricity in multiferroic $BiCrO_3$ epitaxial films," Appl. Phys. Lett. 89, 162904 (2006).

[93] N. A. Hill and K. M. Rabe, "First-principles investigation of ferromagnetism and ferroelectricity in bismuth manganite," Phys. Rev. B 59, 8759 (1999).

[94] P. Baettig, R. Seshadri and N. A. Spaldin, "Anti-polarity in ideal $BiMnO_3$," J. Am. Chem. Soc. 129, 9854 (2007).

[95] R. Ranjan, D. Pandey, N. P. Lalla, "Novel features of $Sr_{1-x}Ca_xTiO_3$ phase diagram: Evidence for competing antiferroelectric and ferroelectric interactions," Phys. Rev. Lett. 84, 3726 (2000).

[96] A. A. Bokov, I. P. Raevskii and V. G. Smotrakov, Sov. Phys. Solid State 25, 1168 (1983).

[97] A. V. Turik et al., Sov. Phys. Solid State 27, 1686 (1985).

[98] P. Groves, "Structural phase transitions and long-range order in ferroelectric perovskite lead indium niobate," J. Phys. C 19, 111 (1986); P. Groves, "The influence of B-site cation order on the phase transition behaviour of antiferroelectric lead indium niobate," J. Phys. C 19, 5103 (1986).

[99] C. A. Randall, D. J. Barber, P. Groves and R. W. Whatmore, "TEM study of the disorder-order perovskite, $Pb(In_{1/2}Nb_{1/2}O_3$," J. Mater. Sci. 23, 3678 (1988).

[100] M. F. Kuprianova, A. V. Turika, S. M. Zaitseva and E. G. Fesenkoa, "Phase transitions in $PbNb_{0.5}B_{0.5}O_3$ (B=Sc, In)," Phase Transitions 4, 65 (1983).

[101] N. Yasuda and H. Inagaki, Jpn. J. Appl. Phys. 30, L2050 (1991).

[102] J. R Kwon and W. K. Choo, J. Phys. Cond. Matt. 3, 2147 (1991).

[103] N. Yasuda and J. Konda, "Successive paraelectric-antiferroelectric-ferroelectric phase transitions in highly ordered perovskite lead ytterbium tantalate," Appl. Phys. Lett. 62, 535 (1993).

[104] C. A. Randall, S. A. Markgraf, A. S. Bhalla, and K. Baba-Kishi, "Incommensurate structures in highly ordered complex perovskites $Pb(Co_{1/2}W_{1/2}O_3$ and $Pb(Sc_{1/2}Ta_{1/2}O_3$," Phys. Rev. B 40, 413 (1989).

[105] K. Baba-Kishi and D. J. Barber, "Transmission electron microscope studies of phase transitions in single crystals and ceramics of ferroelectric $Pb(Sc_{1/2}Ta_{1/2})O_3$," Appl. Crystallogr. 23, 43 (1990).

[106] J. Y. Yi and J. K. Lee, "Stabilized antiferroelectric phase in lanthanum-doped $Na(Bi_{1/2}Ti_{1/2})O_3$," J. Phys. D. 44, 415302 (2011).

[107] D. D. Khalyavin, A. N. Salak, N. P. Vyshatko, A. B. Lopes, N. M. Olekhnovich, A. V. Pushkarev, I. I. Maroz, and Y. V. Radyush, "Crystal structure of metastable perovskite $Bi(Mg_{1/2}Ti_{1/2})O_3$: Bi-based structural analogue of antiferroelectric $PbZrO_3$," Chem. Mater. 18, 5104 (2006).

[108] S. T. Zhang, A. B. Kounga, W. Jo, C. Jamin, K. Seifert, T. Granzow, J. Rodel and D. Damjanovic, "High-strain lead-free antiferroelectric electrostrictors," Adv. Mat. 21, 4716 (2009).

[109] R. C. Miller, E. A. Wood, J. P. Remeika and A. Savage, "$Na(Nb_{1-x}V_x)O_x$ system and ferrielectricity," J. Appl. Phys. 33, 1623 (1962).

[110] K. Ueda and J. Kobayashi, "Antiparallel dipole arrangement in tungsten trioxide," Phys. Rev. 1565 (1953).

[111] V. I. Popolitov, A. N. Lobachev and V. F. Peskin, "Antiferroelectrics, ferroelectrics and pyroelectrics of a stibiotantalite structure," Ferroelectrics 40, 9 (1982).

[112] H. Unoki and T. Sakudo, "Dielectric anomaly and improper antiferroelectricity at the Jahn-Teller transitions in rare-earth vanadates," Phys. Rev. Lett. 38, 137 (1977).

[113] H. Schmid and E. Ascher, "Are antiferroelectricity and other physical properties hidden in spinel compounds?" J. Phys. C 7, 2697 (1974).

[114] J. Albers, A. Klopperpieper, H. J. Rother and K. H. Ehses, "Antiferroelectricity in betaine phosphate," phys. stat. sol. 74, 553 (1982).

[115] W. Zhang, "Exceptional dielectric phase transitions in a perovskite-type cage compound," Angew. Chem. Int. Ed. 49, 6608 (2010).

[116] H. Fu and R. E. Cohen, "Polarization rotation mechanism for ultrahigh electromechanical response in single crystal piezoelectrics," Nature 403, 281 (2000).

[117] L. Bellaiche, A. Garcia and D. Vanderbilt, "Electric-field induced polarization paths in $Pb(Zr_{1-x}Ti_x)O_3$ alloys," Phys. Rev. B 64, 060103 (2001).

[118] Z. G. Ye, "Relaxor ferroelectric $Pb(Mg_{1/3}Nb_{2/3})O_3$:

Properties and present understanding," Ferroelectrics 184, 193 (1996).

[119] S. S. N. Bharadwaja and S. B. Krupanidhi, "Growth and study of antiferroelectric lead zirconate thin films by pulsed laser ablation," J. Appl. Phys. 86, 5862 (1999).

[120] P. Ayyub, S. Chattopadhyay, R. Pinto and M. S. Multani, "Ferroelectric behavior in thin films of antiferroelectric materials," Phys. Rev. B 57, R5559 (1998).

[121] K. Yamakawa, S. Trolier-McKinstry, J. P. Dougherty and S. B. Krupanidhi, "Reactive magnetro co-sputtered antiferroelectric lead zirconate thin films," Appl. Phys. Lett. 67, 2014 (1995).

[122] J. Blok, K. M. Rabe and D. Vanderbilt, "Interplay of epitaxial strain and rotations in $PbTiO_3/PbZrO_3$ superlattices from first principles," Phys. Rev. B 84, 205413 (2011).

[123] K. Boldyreva, L. Pintilie, A. Lotnyk, I. B. Misirlioglu, M. Alexe and D. Hesse, "Thickness-driven antiferroelectric-to-ferroelectric phase transition of thin $PbZrO_3$ layers in epitaxial $PbZrO_3/Pb(Zr_{0.8}Ti_{0.2})O_3$ multilayers," Appl. Phys. Lett. 91, 122915 (2007).

[124] B. Jaffe, W. R. Cook, H. Jaffe, *Piezoelectric Ceramics* (Academic Press, 1971) p. 174

[125] K. Yamakawa, K. W. Gachigi, S. Trolier-McKinstry and J. P. Dougherty, "Structural and electrical properties of antiferroelectric lead zirconate thin films prepared by reactive magnetron co-sputtering," J. Mater. Sci 32, 5169 (1997)

[126] B. Xu, N. G. Pai and L. E. Cross, "Lanthanum doped lead zirconate titanate stannate antiferroelectric thin films from acetic acid-based solgel method," Mater. Lett. 34, 157 (1998)

[127] B. Xu, Y. Ye and L. E. Cross,"Dielectric properties and field-induced phase switching of lead zirconate titanate stannate antiferroelectric thick films on silicon substrates," J. Appl. Phys. 87, 2507 (2000)

[128] X. Li, J. Zhai and H. Chen, "$(Pb,La)(Zr,Sn,Ti)O_3$ antiferroelectric thin films grown on $LaNiO_3$-buffered and Pt-buffered silicon substrates by sol-gel processing,"J. Appl. Phys. 97, 024102 (2005)

[129] O. Yoshiro, "Electrooptic ceramic material," United States Patent 3998523, issue date 1976.

[130] J. P. Dougherty, "Cardiac defibrillator with high energy storage antiferroelectric capacitor," United States Patent 5545184, issue date 1996.

[131] L. Zhu and Q. Wang, "Novel ferroelectric polymers for high energy density and low loss dielectrics," Macromolecules 45, 2937 (2012).

[132] W. Pan, Q. Zhang, A. Bhalla and L. E. Cross, "Field-forced antiferroelectric-to-ferroelectric switching in modified lead zirconate titanate stannate ceramics," J. Amer. Cer. Soc. 72, 1455 (1989)

[133] S. T. Zhang, A. B. Kounga, E. Aulbach, H. Ehrenberg and J. Rodel, "Giant strain in lead-free piezoceramics $Bi_{0.5}Na_{0.5}TiO_3BaTiO_3K_{0.5}Na_{0.5}NbO_3$ system" Appl. Phys. Lett. 91, 112906 (2007).

[134] J. W. Bennett, K. F. Garrity, K. M. Rabe and D. Vanderbilt, Orthorhombic ABC semiconductors as antiferroelectrics, to be published in Physical Review Letters.

[135] N. Ray and U. V. Waghmare, "Coupling between magnetic ordering and structural instabilities in perovskite biferroics: A first-principles study," Phys. Rev. B 77, 134112 (2008).

[136] I. Suzuki and K. Okada, "Phenomenological theory of antiferroelectric transition. IV. Ferrielectric," J. Phys. Soc. Jpn. 45, 1302 (1978).

Phase transitions and antiferroelectricity in BiFeO3 from atomic level simulations. M. Graf1, M. Sepliarsky1, S. Tinte 2 and M.G.Stachiotti1 1 Instituto de FÃsica Rosario, Universidad Nacional de Rosario, Rosario, Argentina 2Instituto de FÃsica del Litoral, Universidad Nacional del Litoral, Santa Fe, Argentina.Â The perovskite oxide BiFeO3 (BFO) is attracting much attention due to its unique properties and potential applications. BFO is the most promising magnetoelectric multiferroic material which displays simultaneously ferroelectric (FE) and ferromagnetic properties coupled at room temperature [1â€“3], and it is expected to have important applications in various fields from spintronics to energy-saving technologies. Antiferroelectricity in oxides: a reexamination. Karin M. Rabe* Department of Physics and Astronomy Rutgers University, Piscataway, NJ 08854 * Corresponding Author: rabe@physics.rutgers.edu. (Dated: December 17, 2012). The fundamental physics of antiferroelectric oxides and their properties are reviewed. First, the diculties in formulating a precise denition of antiferroelectricity are discussed, drawing on pre-vious discussion in the literature. We arrive at the following denition: an antiferroelectric is like a ferroelectric in that its structure is obtained through distortion of a nonpolar Functional oxides are used both as insulators and metallic conductors in key applications across all industrial sectors. This makes them attractive candidates in modern technology ? they make solar cells cheaper, computers more efficient and medical instrumentation more sensitive. Based on recent research, experts in the field describe novel materials, their properties and applications for energy systems, semiconductors, electronics, catalysts and thin films. This monograph is divided into 6 parts which allows the reader to find their topic of interest quickly and efficiently.Â Antiferroelectricity in Oxides a Reexamination. ProbingNanoscale Electronic Conduction. Multiferroics with Magnetoelectric Coupling.